Suppression of Optical Absorption by Electric-Field-Induced Quantum Interference in Coupled Potential Wells

Jérôme Faist, Federico Capasso, Albert L. Hutchinson, Loren Pfeiffer, and Ken W. West
AT&T Bell Laboratories, Murray Hill, New Jersey 07974
(Received 18 August 1993)

A new quantum interference phenomenon in optical absorption is reported. This effect manifests itself in a striking suppression of the absorption coefficient as a function of the electric field concomitant with a negligible Stark shift of the transition in suitably designed coupled-quantum-well semiconductors. This phenomenon, which does not arise from a reduced overlap of the final and initial states of the transition, is shown to be caused by quantum interference between two spatially separated transitions. The basic and general nature of this mechanism could be exploited in other artificially structured materials as well.

PACS numbers: 78.66.Fd, 78.20.Jq

Quantum interference effects in the absorption of atoms and molecules have been investigated since the seminal work of Fano on continuum resonances [1]. Recent examples include interference between multiple absorption pathways in two-photon absorption [2] and in molecular dissociation [3], absorption cancellation in dressed three level atomic systems which may lead to lasing without inversion [4], and the production of a large index of refraction with vanishing absorption by atoms prepared in a coherent superposition of an excited state doublet [5].

The development of molecular beam epitaxy (MBE) [6] and band-gap engineering [7] has made possible the design and realization of quantum semiconductor structures with new and unusual optical properties [8]. Of particular interest in this respect are quantum dots [9] and coupled-quantum-well structures [10,11] which behave, respectively, as giant artificial atoms and "quasimolecules" with dipole matrix elements between electronic states many orders of magnitude larger than atomic and molecular ones.

In this paper we report the design and demonstration of a coupled-quantum-well semiconductor exhibiting a new quantum interference effect in absorption between electronic states. This phenomenon manifests itself in a striking electric-field-induced suppression of intersubband absorption, accompanied by a negligible Stark shift of the corresponding transition. As such the large modulation of the dipole matrix element in our effect does not originate from a reduced overlap between the wave functions as in the case of the quantum confined Stark effect [12] and of the linear Stark effect of interband transitions in coupled quantum wells [13], but has its subtle origin in the quantum interference between the two coupled wells.

The sample, grown by MBE on a semi-insulating GaAs substrate, comprises fifty modulation-doped coupled quantum wells. Each period consists of two GaAs wells, respectively 62 and 72 Å thick, separated by a 20 Å $Al_{0.33}Ga_{0.67}As$ barrier. The coupled-well periods are separated by a 1450 Å $Al_{0.33}Ga_{0.67}As$ spacer layer. To supply the electron charge in the wells, a δ-doped Si layer ($1\times10^{12}/cm^2$) is inserted in the spacer layers to ensure a symmetric charge transfer [14]. The growth sequence starts and ends with a GaAs contact layer, doped with Si to $n=1\times10^{18}$ cm^{-3}.

Figure 1(a) shows the conduction band diagram of a period of the sample at zero bias. Indicated are the energy levels and the modulus squared of the wave functions.

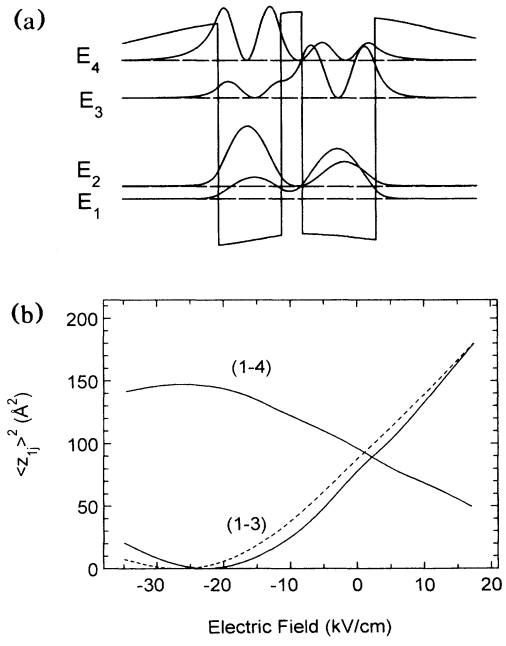

FIG. 1. (a) The energy band diagram of a single period of the GaAs/$Al_{0.33}Ga_{0.67}As$ modulation-doped structure. Shown are the positions of the calculated energy subbands and the corresponding modulus squared of the wave functions. We computed $E_1=63$ meV, $E_2=80$ meV, $E_3=198$ meV, and $E_4=250$ meV. (b) Square of the intersubband dipole matrix element $(z_{13})^2$ and $(z_{14})^2$ (as indicated) computed as a function of the electric field. Dotted line: tight-binding model for $(z_{13})^2$.

0031-9007/93/71(21)/3573(4)$06.00

The energy levels and wave functions are computed by solving Schrödinger's and Poisson's equations in the envelope-function formalism [15,16]. The exchange interaction (Slater term) is included in the local-density approximation [17].

To get a better insight into the behavior of the coupled-well system as a function of the applied electric field, let us first consider the two quantum wells, denoted here as wells a and b, coupled by the barrier in a tight-binding approach [15]. In such a model, the calculated wave functions ψ_i $(i=1,\ldots,4)$ of this system are expanded in terms of the eigenfunctions $\varphi^{a,b}_{1,2}$ of the first two bound states 1,2 of the two isolated wells. In the tight-binding approximation, the dipole matrix element $z_{1i}=\langle\psi_1|z|\psi_i\rangle$ $(i=3,4)$ between the first and the third or fourth state of the coupled-well system can now be written as the sum of the contribution from the two wells a and b,

$$z_{1i}=\langle\psi_1|\varphi^a_1\rangle\langle\psi_i|\varphi^a_2\rangle z^a_{12}+\langle\psi_1|\varphi^b_1\rangle\langle\psi_i|\varphi^b_2\rangle z^b_{12}\,, \qquad (1)$$

where z^a_{12} and z^b_{12} are the transition matrix elements computed for the isolated wells. As ψ_1 is the ground state of the system, $\langle\psi_1|\varphi^a_1\rangle$ and $\langle\psi_1|\varphi^b_1\rangle$ have the same sign. On the contrary, since the second excited state ψ_3 crosses zero twice and is constructed from the antisymmetric wave functions $\varphi^{a,b}_2$, $\langle\psi_3|\varphi^a_2\rangle$ and $\langle\psi_3|\varphi^a_2\rangle$ have opposite signs. Therefore, if we consider a transition between the first and third state of the coupled-well system, the two terms of Eq. (1) have opposite signs. One thus expects large values of z_{13} for large absolute values of the electric field where both wave functions are localized in either well a or b [first or last term of Eq. (1) dominates] and a null for some intermediate value of the electric field. At this field the absorption will be suppressed. This behavior is clearly apparent in Fig. 1(b), where we display $(z_{13})^2$ as given by Eq. (1) along with the exact calculation, using the parameters of the sample. As expected, z_{13} decreases with the applied field and has a null for an electric field of -22 kV/cm. The tight-binding result is in good agreement with the exact computation in which z_{13} is directly computed from the wave functions $\psi_{1,3}$, supporting our interpretation of this effect as an interference phenomenon. The self-consistent potential takes into account the screening of the applied electric field by the charges inside the coupled wells. The interference effect still occurs even if the self-consistent potential is neglected, although at a different applied field. It is important to note that the suppression of the dipole matrix element $(z_{13}=0)$ does not arise from the parity selection rule, since for all electric fields the wave functions ψ_1 and ψ_3 do not have a well-defined parity.

The interference phenomenon occurs for the 1-3 transition because the two terms in Eq. (1) have opposite signs. On the contrary, as $\langle\psi_4|\varphi^a_2\rangle$ and $\langle\psi_4|\varphi^b_2\rangle$ have the same sign, the two terms of Eq. (1) for the 1-4 transition add constructively. For large values of the electric field, the ground state wave function ψ_1 will be localized in one well and ψ_4 in the other. The two wave functions ψ_1 and ψ_4 now having a small overlap, the resulting dipole matrix element z_{14} will be small. This behavior appears clearly in Fig. 1 where $(z_{14})^2$ is displayed as a function of the applied field. z_{14} is maximum at about -22 kV/cm and decreases for positive fields or larger negative fields.

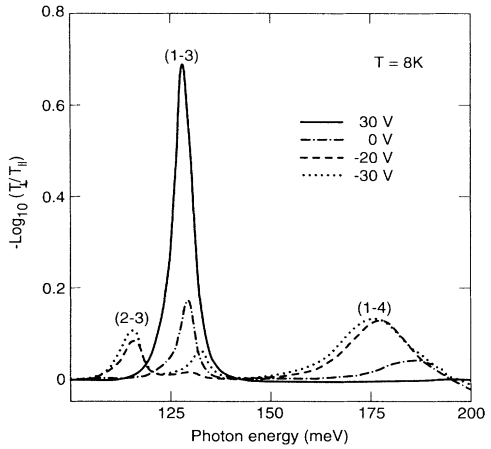

FIG. 2. Intersubband absorption spectra in a two-pass waveguide at $T=8$ K for different applied biases, as indicated. The absorbance for polarization parallel to the plane of the layers $(-\log_{10}T_{\parallel})$ is subtracted from the absorbance normal to the plane of the layer $(-\log_{10}T_{\perp})$ to remove instrumental, substrate, and free carrier absorption contributions. A strong modulation of the absorption of the 1-3 and 1-4 transitions is observed.

For the experiments, the samples were processed into square mesas (800 μm side) and Ohmic contacts were provided to the n^+ contact layers. They were then cleaved in strips and the cleaved edges were polished at 45° to provide a two-pass waveguide. The absorption spectra were measured with a Nicolet 800 Fourier transform infrared spectrometer (FTIR) using this wedge waveguide geometry. In Fig. 2 the low-temperature absorption spectra are shown for different applied biases. Positive bias refers to the band diagram configuration in which the thick well is lowered below the thin well. The height of the absorption peak corresponding to the 1-3 transition (136 meV) decreases regularly when the applied bias U_b is changed from 30 to -20 V, has a minimum at this value, and rises again if the bias is decreased further to -30 V. At -20 V, the integrated absorption of the peak has decreased to 1.6% of its value at 30 V. Meanwhile, as shown also in Fig. 2, the 1-3 transition energy has changed by less than 1 meV in the same bias range. Thus the modulation of the absorption is not due to an electric-field-induced shift of the transition like in the Stark effect. As expected from the computations, the 1-4 transition has the opposite behavior; its oscillator strength is maximum for $U_b=20$ V and not observable anymore at 30 V. Although there is a clear exchange of oscillator strengths between the 1-4 and 1-3 transitions as

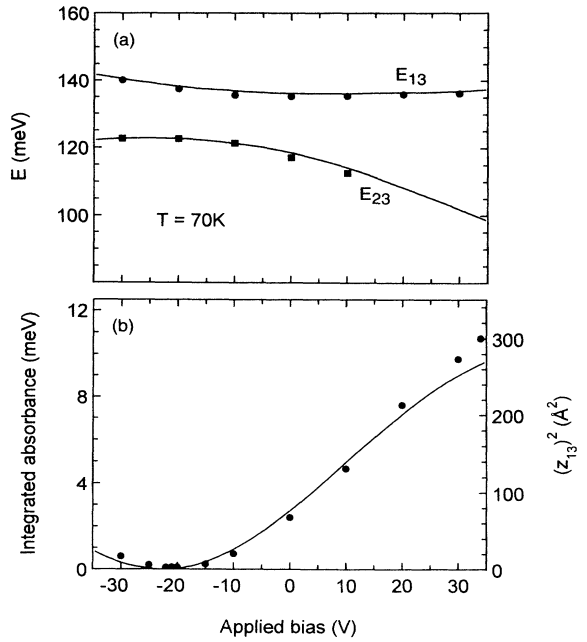

FIG. 3. (a) Comparison between the measured and calculated (solid lines) E_{13} and E_{23} transition energies. In order to track E_{23} for a larger range of applied fields, the temperature was raised to 70 K to induce a thermal population of the second level. (b) Square of the transition matrix element $(z_{13})^2$ (right axis), as derived experimentally from the integrated absorbance below the 1-3 peak (left axis) at $T=8$ K. The solid line is the calculated value.

a function of bias, the sum of the oscillator strength of these two transitions is not constant because the 1-2 transition also exchanges oscillator strength with the 1-3 and 1-4 transitions. The energy of the 1-2 transition has its minimum near $U_b = -20$ V. At this bias, the second state drops slightly below the Fermi energy, allowing the observation of a third peak at $h\nu = 124$ meV corresponding to the 2-3 transition. However, by evaluating the electron sheet density $n_s^{(2)}$ in the second state from the integrated absorbance below the 2-3 peak, we find $n_s^{(2)} = 3\times10^{10}$ cm^{-2}, less than 10% of the ground state density. Therefore, the population of the second state has a negligible impact on the modulation of the 1-3 absorption.

The characteristic anticrossing of the first two levels as a function of the applied bias is clearly apparent from Fig. 3(a) where the measured transition energies E_{13} and E_{23} are reported along with the theoretical predictions using the full self-consistent model. As shown in Fig. 3, the experimental points are in excellent agreement with the theory. In Fig. 3(b), $(z_{13})^2$ is derived from the measured integrated absorption [18] and the nominal electron sheet density $n_s = 5\times10^{11}$ cm^{-2}, as obtained from prior calibration of the MBE system [14] on similar samples. The agreement with the theoretical prediction is excellent. As expected, $(z_{13})^2$ decreases first as the field is increased, has a minimum for $U_b = -20$ V, and then rises again.

As expected from an interference phenomenon, the amplitude of the wave functions in each well enter in Eq. (1), and these wave functions must remain coherent across the coupled-well system. The importance of this coherence has recently been demonstrated in the generation of terahertz radiation from charge oscillation in coupled wells [19] and in quantum transport phenomena such as the "resistance resonance" [20]. A sufficient amount of disorder will localize the wave functions in either well and completely destroy the interference effect. Indeed, this localization effect has recently been observed [21]. In this work, the absorption of a coupled-well system with a thicker tunnel barrier (40 Å) is reported as a function of the applied field. The wave functions are localized in the two wells and no modulation of the dipole transition element z_{13} is observed [21]. The modulation of the absorption is entirely due to a transfer of electrons from the ground state of one well to the ground state of the other well having a different transition energy.

In conclusion, we have demonstrated a new quantum interference effect in optical absorption which results in the electric-field-induced suppression of the latter. The large modulation of the transition matrix element could be useful in modulator applications. The basic nature of this mechanism could possibly also be exploited in other material systems such as organic quantum wells [22].

It is a pleasure to acknowledge many stimulating discussions with C. Sirtori and P. von Allmen.

[1] U. Fano, Phys. Rev. **124**, 1866 (1961).
[2] R. B. Stewart and G. J. Diebold, Phys. Rev. A **34**, 2547 (1986).
[3] M. Class-Manjean, H. Frohlich, and J. A. Beskick, Phys. Rev. Lett. **61**, 157 (1988).
[4] S. E. Harris, Phys. Rev. Lett. **62**, 1033 (1989).
[5] M. O. Scully, Phys. Rev. Lett. **67**, 1855 (1991).
[6] A. Y. Cho, J. Cryst. Growth **111**, 1 (1991).
[7] F. Capasso, MRS Bull. **16**, 23 (1991).
[8] For a recent review, see Phys. Today **46**, No. 6 (1993).
[9] D. Heitmann and J. P. Kotthaus, Phys. Today **46**, No. 6, 56 (1993).
[10] C. Sirtori, F. Capasso, D. L. Sivco, and A. Y. Cho, Phys. Rev. Lett. **68**, 1010 (1992).
[11] C. Sirtori, F. Capasso, D. L. Sivco, and A. Y. Cho, Appl. Phys. Lett. **60**, 2678 (1992).
[12] W. Chen and T. G. Andersson, Semicond. Sci. Technol. **7**, 828 (1992).
[13] H. Q. Le, J. J. Zayhowski, and W. D. Goodhue, Appl. Phys. Lett. **50**, 1518 (1987).
[14] L. Pfeiffer, E. F. Schubert, and K. W. West, Appl. Phys. Lett. **58**, 2258 (1991).
[15] G. Bastard, *Wave Mechanics Applied to Semiconductor Heterostructures* (les Editions de Physiques, Paris, 1990).
[16] Nonparabolicities were taken into account using the method of D. F. Nelson, R. C. Miller, and D. A. Klein-

mann, Phys. Rev. B **35**, 7770 (1987). The values of the parameters used are $\Delta E_c = 298$ meV, $m_e^*(\mathrm{GaAs}) = 0.067 m_0$, $m_e^*(\mathrm{Al_{0.33}Ga_{0.67}As}) = 0.086 m_0$, and γ(non-parabolicity coefficient) $= 4.9 \times 10^{-19}$ m^2.

[17] The effective Slater term for GaAs is given by $\Delta E = -1.1 \times 10^{-8} n^{1/3}$ eV/cm, where n is the electron volume density.

[18] C. Sirtori, F. Capasso, D. L. Sivco, S. N. G. Chu, and A. Y. Cho, Appl. Phys. Lett. **59**, 2302 (1991).

[19] H. G. Roskos, M. C. Nuss, J. Shah, K. Leo, D. A. B. Miller, A. M. Fox, S. Schmitt-Rink, and K. Köhler, Phys. Rev. Lett. **68**, 2216 (1992).

[20] A. Palevski, F. Beltram, F. Capasso, L. Pfeiffer, and K. W. West, Phys. Rev. Lett. **65**, 1929 (1990).

[21] N. Vodjdani, B. Vinter, V. Berger, E. Bockenhoff, and E. Costar, Appl. Phys. Lett. **59**, 555 (1991).

[22] J. F. Lam, S. R. Forrest, and G. L. Tangonan, Phys. Rev. Lett. **66**, 1614 (1991).